JOURNAL OF THE ROYAL SOCIETY Interface

Genomic expression of mesenchymal stem cells to altered nanoscale topographies

Matthew J Dalby, Abhay Andar, Abhijit Nag, Stanley Affrossman, Rahul Tare, Sara McFarlane and Richard O.C Oreffo

J. R. Soc. Interface 2008 **5**, 1055-1065
doi: 10.1098/rsif.2008.0016

JOURNAL OF THE ROYAL SOCIETY Interface

J. R. Soc. Interface (2008) **5**, 1055–1065
doi:10.1098/rsif.2008.0016
Published online 12 February 2008

Genomic expression of mesenchymal stem cells to altered nanoscale topographies

Matthew J. Dalby[1,*], Abhay Andar[1], Abhijit Nag[1], Stanley Affrossman[2], Rahul Tare[3], Sara McFarlane[4] and Richard O. C. Oreffo[3]

[1]*Centre for Cell Engineering, Joseph Black Building, Institute of Biomedical and Life Sciences, University of Glasgow, Glasgow G12 8QQ, UK*
[2]*Department of Pure and Applied Chemistry, Thomas Graham Building, University of Strathclyde, Cathedral Street, Glasgow G1 1XL, UK*
[3]*Bone and Joint Research Group, Centre for Human Development, Stem Cells and Regeneration, Institute of Developmental Sciences, University of Southampton, Southampton SO16 6YD, UK*
[4]*Centre for Cell Engineering, Department of Electronics and Electrical Engineering, Rankine Building, University of Glasgow, Glasgow G12 8QQ, UK*

The understanding of cellular response to the shape of their environment would be of benefit in the development of artificial extracellular environments for potential use in the production of biomimetic surfaces. Specifically, the understanding of how cues from the extracellular environment can be used to understand stem cell differentiation would be of special interest in regenerative medicine.

In this paper, the genetic profile of mesenchymal stem cells cultured on two osteogenic nanoscale topographies (pitted surface versus raised islands) are compared with cells treated with dexamethasone, a corticosteroid routinely used to stimulate bone formation in culture from mesenchymal stem cells, using 19k gene microarrays as well as 101 gene arrays specific for osteoblast and endothelial biology.

The current studies show that by altering the shape of the matrix a cell response (genomic profile) similar to that achieved with chemical stimulation can be elicited. Here, we show that bone formation can be achieved with efficiency similar to that of dexamethasone with the added benefit that endothelial cell development is not inhibited. We further show that the mechanism of action of the topographies and dexamethasone differs. This could have an implication for tissue engineering in which a simultaneous, targeted, development of a tissue, such as bone, without the suppression of angiogenesis to supply nutrients to the new tissue is required. The results further demonstrate that perhaps the shape of the extracellular matrix is critical to tissue development.

Keywords: nanobioscience; mesenchymal stem cells; osteogenesis; differentiation; nanotopography; microarray

1. INTRODUCTION

An array of studies over many years indicate that cells respond to the shape of their environment through changes in morphology; this is commonly termed contact guidance (Weiss & Garber 1952; Curtis & Varde 1964). Initial work using microtopography showed that other cellular responses include migration, adhesion, cytoskeletal organization and gene regulation (Clark *et al.* 1987, 1990; Wójciak-Stothard *et al.* 1995, 1996). More recently, it has been shown that nanoscale topography can have similar effects (Curtis & Wilkinson 2001) as determined with a large number of terminally differentiated cell types including fibroblasts (Dalby *et al.* 2002*b*, 2004*a*,*d*), endothelial cells (Dalby *et al.* 2002*a*), epithelial cells (Andersson *et al.* 2003*a*–*c*), neurons (Clark *et al.* 1991; Rajnicek & McCaig 1997; Rajnicek *et al.* 1997) and macrophages (Wójciak-Stothard *et al.* 1996).

We have previously published studies that demonstrate the formation of bone nodules on highly defined topographies with nanoscale depths and on random nanotopographies (Dalby *et al.* 2006*a*,*b*). The formation of bone nodules is an indicator of an enhanced bone-forming potential as the bone mineral (apatite formed by calcium phosphates similar to synthetic hydroxyapatite) is formed within the nodules. In an extension of this work, we consider here whether some of these topographies could change stem cell differentiation through changes in genome regulation. In this

*Author for correspondence (m.dalby@bio.gla.ac.uk).

Electronic supplementary material is available at http://dx.doi.org/10.1098/rsif.2008.0016 or via http://journals.royalsociety.org.

Received 16 January 2008
Accepted 21 January 2008

study, stro-1-immunoselected mesenchymal stem cells (MSCs) were cultured on nanotopographies selected from the above studies and microarray was used to examine similarities in the patterns of gene expression when compared with cells treated with dexamethasone, a glucocorticoid steroid commonly used to increase MSC differentiation to osteoblasts.

stro-1 has been shown to be a marker of multipotent cells extracted from the bone marrow, termed MSCs (Oreffo *et al.* 1998; Triffitt & Oreffo 1998). A wealth of evidence indicates that mesenchymal stem cell multipotency can give rise to cells of the adipogenic (fat), chondrogenic (cartilage), osteoblastic (bone), myoblastic (muscle), endothelial and mesothelial (vasculature) and fibroblastic and reticular (connective tissue) lineages and generate intermediate progenitors with an apparent degree of plasticity (Bianco *et al.* 2001; Oreffo *et al.* 2005). Thus, MSCs give rise to a hierarchy of bone cell populations with a number of developmental stages: MSC, determined osteoprogenitor cell, preosteoblast, osteoblast and, ultimately, osteocyte (Friedenstein 1976; Bianco & Robey 2001; Oreffo *et al.* 2005).

The cells were selected as an ideal orthopaedic repair material would have to influence this osteoprogenitor cell mix *in vivo* to differentiate into mature osteoblasts rather than connective tissue cell types. The mature osteoblasts would then produce the appropriate extracellular matrix collagen type I and apatite mineral required for new bone formation.

Advances in microarray bioinformatics, such as Ingenuity Pathway Analysis (IPA), as used here, have allowed a move away from gene fishing and the problems associated with microarray reliability. Rather, it is now possible to consider gene responses as groups and functions. To do this, a primary statistic is first generated, such as rank product (RP) (Breitling *et al.* 2004) which considers fold-change, false discovery rate (FDR) and array spot quality and has traditionally been used to produce, for example, dendrographs as used initially in this study. Instead, the ranked results are used to feed robust changes into pathway and functional databases, and thus an integrative rather than an individual approach is used. This approach was used here in order to locate signalling pathways of interest and then to highlight downstream function.

While it seems more appropriate to use large arrays to search for patterns or groups of gene activity, arrays can also be used to observe individual gene changes. Reliable oligo (short, highly specific, DNA-expressed sequence tags) macroarrays have been used here to look for individual 'hits' in specialized function analysis.

The selected nanoscale topographies were produced by two methods. Firstly, polymer demixing where blends of polystyrene (PS) and polybromostyrene in a toluene solvent were spin coated on to Si wafers. Depending on the polymer blend, spin speed and the ratio of polymer to solvent, different topographies were produced. In this study we consider 33 nm high islands. Secondly, photolithography, routinely used in the production of microchips, has been used to produce pits with a depth of 400 nm and a diameter of 40 µm (similar in scale to osteoclastic resorption pits). Both have been shown to produce increased levels of osteocalcin (a bone matrix-specific protein) in osteoprogenitor cells when compared with planar surfaces (Dalby *et al.* 2006*a*,*b*).

To provide directly comparable topographies that have been fabricated by different routes in different bulk materials, directly comparable Ni intermediaries were used. These are negatives of the master materials manufactured by electroplating. These shims can then be used to emboss positive replicas into polymers like polymethylmethacrylate (PMMA). This technique can produce replicas with 5 nm resolution.

The capacity to elicit desirable patterns of stem cell differentiation offers clear benefits in regenerative medicine, specifically tissue engineering. A key goal of tissue engineering is the production of bioactive scaffold materials that will support a new tissue formation to replace diseased or damaged tissue. Current strategies include the use of factors, such as dexamethasone, for stem cell stimulation, with the limitations therein for *in vivo* translation.

A further goal in tissue engineering is angiogenesis. The ability to engineer complicated tissues in the laboratory from specialized cells is currently limited as a consequence of robust angiogenic protocols. This is the reason why stem cells, especially autologous tissue stem cells, have the potential to underpin the whole tissue engineering discipline. To engineer new bone, ideally an enriched osteoblast population would be stimulated from the stem cells, in addition to which endothelial cells capable of forming new capillaries within the nascent tissue would also be required.

In this study, three types of microarray were used. Firstly a 19k gene general cDNA array, then a 101 gene osteospecific oligo macroarray and finally a 101 gene endothelial-specific macroarray. The MSCs were cultured for 14 days (and 28 days for pathway analysis) as this is the time point when proliferation slows and large-scale differentiation commences (Stein & Lian 1993).

2. MATERIAL AND METHODS

2.1. Materials

2.1.1. Photolithography. Three silicon wafers were cleaned under acetone in an ultrasonic bath for 5 min. They were then rinsed thoroughly in reverse osmosis water (ROH_2O) and blow-dried under air flow. They were first spun with a primer for 30 s at 4000*g* and again with S1818 photoresist for 30 s at 4000*g* and baked for 30 min at 90°C. The resulting layer was measured to be 1.8 µm in thickness. The photoresist layer was exposed to UV light through a chrome mask featuring an array of pits on a Karl Suss MA6 mask aligner for 3.8 s. Then, the resist layer was developed for 75 s in 50 : 50 Microposit developer and ROH_2O.

The specific design pattern, in this case circles, was achieved by reactive ion etching using the exposed photoresist as a mask. The silicon substrate was etched in the silicon tetrachloride gas plasma of a Plasmalab System 100 machine (gas flow, 18 sccm; pressure, 9 mTorr; rf power, 250 W; DC bias, −300 V). The wafer was etched individually at 7 min at a nominal etch rate of 18 nm min^{-1}. It was then stripped of resist

in an acetone ultrasound bath for 5 min, followed by a 5 min soak in concentrated sulphuric acid/hydrogen peroxide mixture before rinsing thoroughly in ROH_2O and drying in air flow.

2.1.2. Polymer demixing. PS (Aldrich secondary standard, UK) and poly(4-bromostyrene) (PBrS; Aldrich, UK) were each reprecipitated twice, to remove low molecular weight materials before use. In order to produce the test materials, a 60% PBrS/40% PS w/w blend was used to form nanoscale 'islands'. A spin speed of 3000*g* and a total polymer concentration of 3% in toluene were used to produce 55 nm high features.

2.1.3. Nickel shims. Nickel dies were made directly from the patterned resist samples. A thin (50 nm) layer of Ni–V was sputter coated on the samples. This layer acted as an electrode in the subsequent electroplating process. The dies were plated to a thickness of approximately 300 μm.

Once returned from the plater, the nickel shims were cleaned by firstly stripping the protective polyurethane coating using chloroform in an ultrasound bath for 10–15 min. Secondly, silicon residue was stripped by being wet etched in 25% potassium hydroxide at 80°C for 1 hour. Shims were rinsed thoroughly in ROH_2O and then air dried. The shims were finally trimmed to approximately 30×30 mm sizes using a metal guillotine.

Imprints of the nickel shims into PMMA was achieved using an Obducat nanoimprinter (temperature, 180°C; pressure, 15 bar; time, 300 s). The imprints were trimmed and depth measurements (Dektak) were made of a random sample from each etch depth category. Random samples were taken for inspection by atomic force microscopy or scanning electron microscopy.

Planar PMMA (Ra of 1.17 nm over 10 mm) was used as a control substrate.

2.1.4. Cell extraction and culture. Human osteoprogenitors were extracted from bone marrow samples obtained from haematologically normal patients undergoing routine hip replacement surgery as described previously (Yang *et al.* 2003). These cells represent the adherent bone marrow stromal cell fraction. MSCs were selected from the osteoprogenitor population using stro-1 antibody and magnetic cell sorting (Howard *et al.* 2002; Mirmalek-Sani *et al.* 2006), as described previously. MSCs were maintained in a basal medium (10% FCS/αMEM, Life Technologies, UK) at 37°C with 5% CO_2 under humid conditions. The cells were trypsinized from a culture flask before counting with a haemocytometer for seeding onto the materials. To trypsinize, the cells were washed with HEPES/saline and detached for 5 min in 0.06% trypsin in versine. The trypsin was quenched with complete medium before centrifugation, counting and seeding.

The cells were seeded onto the materials at 1×10^4 cells cm^{-2} and the medium changed twice weekly. For microarray and macroarray analysis, one set of cells was cultured with a similar medium containing DEX (10 nM) and L-ascorbic acid (150 μg ml^{-1}).

It is noted that cells from two patients were used (both at passage 1). One set for the microarrays and another for the macroarrays. It is further noted that our initial published findings describing the histochemical observation of osteoprogenitor cells on the materials were performed with cells from two other patients (Dalby *et al.* 2006*a*,*b*).

2.1.5. Microarrays. Individual gene expression changes were detected using spotted DNA microarrays. The arrays were printed with 19k distinct human transcripts obtained from the Ontario Cancer Institute Microarray Centre (http://www.microarrays.ca). Complete protocols for the generation of fluorescence labelled samples from whole cell RNA, hybridization to DNA microarrays and data processing can be found at this website (and has been previously published; Dalby *et al.* 2003). The cells were cultured for 14 days. At this point, the cells were lysed and total RNA was extracted using an Absolutely RNA kit (Stratagene, UK). Next, mRNA was extracted using pellet paint. The resulting mRNA was amplified using a GeneChip Eukaryotic Small Sample Target Labelling Assay Version II (Affymetix, UK) using the Two Cycle cDNA Synthesis method. Two micrograms of mRNA were hybridized to the arrays (four replicates for each sample) after reverse transcription with Alexa 555-dUTP for test and Alexa 647-dUTP for control RNA (Invitrogen, UK). Data were exported and log normalized into a spreadsheet before cluster analysis using published protocols (Eisen *et al.* 1998).

IPA was used via a licence to Ingenuity Systems, (www.ingenuity.com) in order to identify (i) canonical signalling pathways and (ii) functional pathways. Here, the RP-generated gene lists cut at 50% FDR were uploaded into the IPA server as input data. IPA uses pathway libraries derived from the scientific literature. Statistics for functional analysis were performed by Fischer's exact test (as done automatically by the software with $p<0.05$ considered significant).

2.1.6. Macroarrays. For specific observation of osteoblastic and endothelial differentiation, GEoligoarrays (Tebu-bio, UK) were used according to the manufacturer's instructions. In brief, the cells were seeded onto the materials (three replicates) at 1×10^4 cells per ml and the medium changed twice weekly for 14 days. At this point, the cells were lysed and total RNA was extracted using an Absolutely RNA kit (Stratagene, UK). The control and test RNAs were reverse transcribed with biotin-UTP (InVitrogen, UK). Finally, the RNAs were hybridized to the arrays and exposed to an X-ray film for detection. The online software from Tebu-Bio was used for the detection of expressed genes. Please note that, owing to a restricted sample size, fully quantitative analysis was not viable. Thus, a semi-quantitative approach has been used whereby positive 'hits' were recorded on each array.

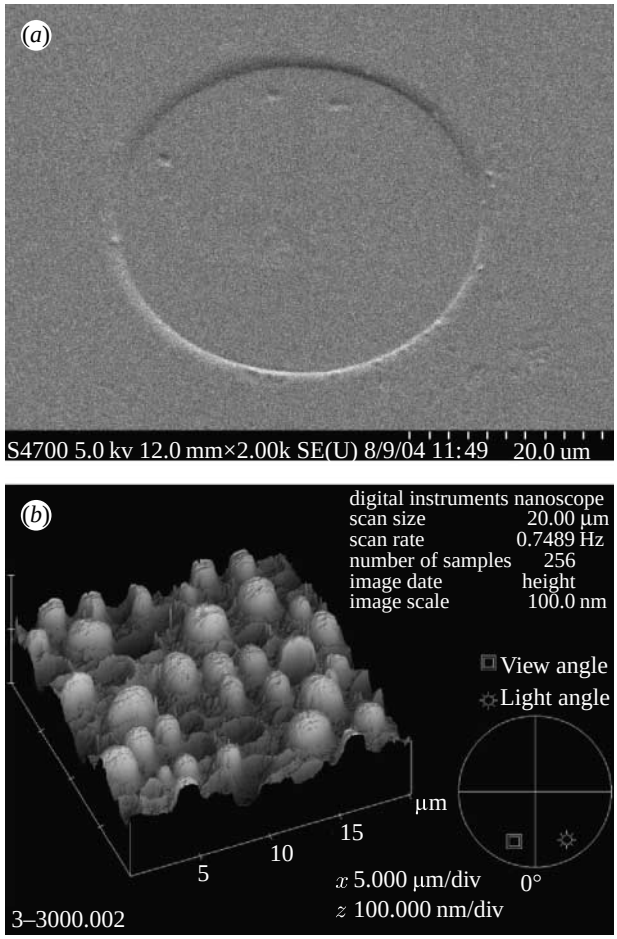

Figure 1. Images of the test nanotopographies. (*a*) Scanning electron microscopic image of a 40 µm wide, 400 nm deep pit produced by photolithography embossed into PMMA (40 : 400). (*b*) Atomic force microscopic image of 33 nm high islands produced by polymer demixing embossed into PMMA (3% : 3000).

3. RESULTS

Photolithographically produced pits were reproduced in PMMA with good fidelity. The originals had a diameter of 40 µm and a depth of 400 nm. The imprints had a diameter of 40 µm and a depth of 362 nm—referred to as 40 : 400, as dimensions derived from the original diameter : original depth (images of imprints are shown in figure 1*a*).

In contrast, polymer demixed islands did not reproduce with such good fidelity. The originals had a mean height of 55 nm. The imprints had a height of 33 nm. These samples are referred to as 3% : 3000 derived from total polymer : spin speed (images of imprints shown in figure 1*b*). Planar PMMA controls had an Ra (roughness average) value of 1.17 nm over 10 mm.

Microarray results and cluster analysis (Eisen *et al.* 1998) comparing MSC gene regulations for 40 : 400 and 3% : 3000 demonstrated at-a-glance similarities/differences in gene profiles that are displayed in the electronic supplementary material. The most notable trend was for broad upregulation of the genome in MSCs cultured on 3% : 3000 and with dexamethasone. At the same time the regulation of genes in MSCs cultured on 40 : 400 was rather more in flux and, while a large number of similarly upregulated areas were noted, there was also a mix of up- and downregulations (see figure S1, electronic supplementary material). Another predominant trend was that of downregulation on the topographies and upregulation with dexamethasone treatment (figure S2, electronic supplementary material).

In order to look into these changes in genomic regulation, IPA was used. Ingenuity pathway canonical analysis (well-defined cellular signalling cascades) and functional analysis showed a broad number of similarities and some differences between MSCs stimulated by the two test topographies compared with each other and with dexamethasone treatment (figure 2). It is noted at this point that the pathway analysis does not indicate the direction of regulation, rather just that statistically significant changes have been noted for a number of genes in the pathway. To look more in depth, the individual pathways need to be viewed (as is done in the electronic supplementary material for selected pathways).

A number of topography-only (i.e. not significantly influenced by dexamethasone) pathways were noted, including p38 mitogen-activated protein kinase (MAPK), actin cytoskeletal signalling, fibroblast growth factor (FGF) and platelet-derived growth factor (PDGF) (note that although the FGF and PDGF pathways were below the $p<0.05$ significance threshold they are considered here as there was no output for dexamethasone-treated cells and that is of clear interest to this study; figure 2*a*).

p38 MAPK is involved in inflammation and apoptosis (Cook *et al.* 2007; figure 2*a*) and, while the 40 : 400 topography downregulates genes in the cytoplasm, this causes an upregulation of genes in the nucleus. However, 3% : 3000 induces upregulation of cytoplasmic pathways and downregulation of nuclear pathways (figure S3, electronic supplementary material).

Actin is involved in a broad range of signalling events related to focal adhesions, cell motility (cell lamellipodia) and cell sensing of substrate (filopodia; Burridge & Chrzanowska-Wodnicka 1996; figure 2*a*). Figure S4, electronic supplementary material, shows that for MSCs on the 40 : 400, a small number of up- and downregulations were noted within the pathway; however, 3% : 3000 induced a large number of upregulations.

FGF is involved in cell differentiation, proliferation, morphogenesis and angiogenesis (Wilkie 2005). Here, it was shown that while the 40 : 400 topography causes a balance of up- and downregulations in the pathway, the 3% : 3000 topography results mainly in upregulation of the FGF pathway (figure S5, electronic supplementary material) (figure 2*a*).

PDGF is involved in cell proliferation and survival (Ruiz *et al.* 2007). Figure S6, electronic supplementary material, shows that, while culture on the 40 : 400 topography results in a small number of downregulations, culture of MSCs on 3% : 3000 results in a broad number of pathway-associated upregulations (figure 2*a*).

The 3% : 3000 substrate specifically produced statistically significant changes in two pathways in which no genes fits were noted for cells on 40 : 400 and only non-statistically significant outputs for cells

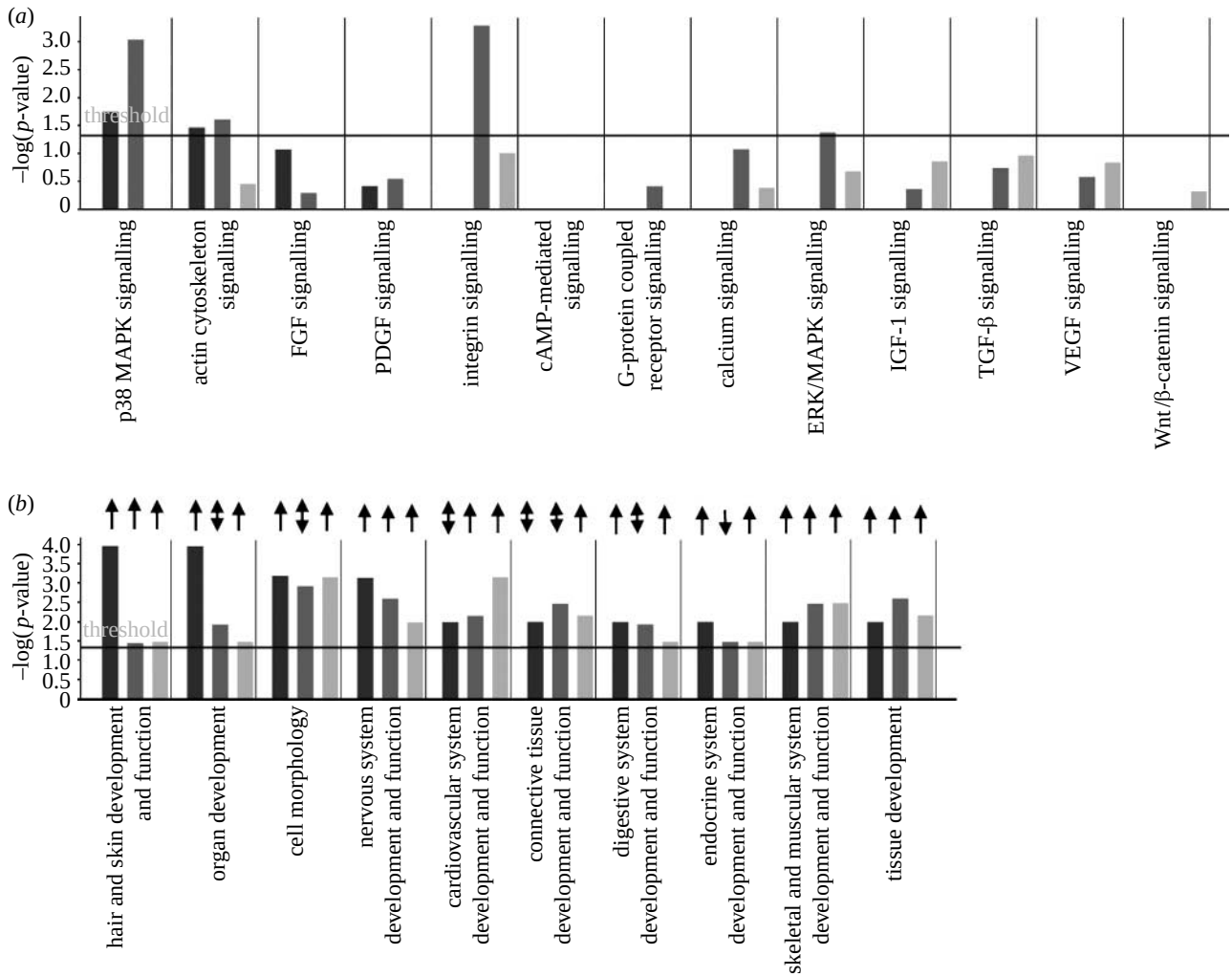

Figure 2. Ingenuity pathway analysis for MSCs cultured on the test topographies for 14 days. (*a*) Canonical pathway analysis for MSCs cultured on the 3% : 3000 and 40 : 400 test substrates compared with cells treated with dexamethasone. (*b*) Functional analysis showing a broad range of functional pathways active in cells in all growth conditions. Arrows indicate the trend of gene regulations within the pathway (up arrow, upregulations; double-headed arrow, balance of up- and downregulations; down arrow, downregulations). The threshold line shows the significance cut-off.

cultured with dexamethasone. These were integrin-related signalling, which has effects on cell adhesion, motility, cytoskeleton and signalling (Burridge & Chrzanowska-Wodnicka 1996), and extracellular receptor kinase (also known as MAPK; ERK, associated with proliferation and differentiation; Dai *et al.* 2007; figure 2*a*). It should be noted at this point that MAPKs fall into several groups and can be broadly classified as p38 MAPKs and ERKs (ERKs contain several MAPK groups). As has been described, the ERKs have roles in proliferation and differentiation and the p38 MAPKs in cell survival.

General upregulation was noted for MSCs cultured on 3% : 3000 and with dexamethasone (non-statistically significant) for integrin signalling. An interplay of up- and downregulations was noted for both 3% : 3000 and dexamethasone treatment (again only statistically significant for alterations to the pathway in cells on the 3% : 3000 topography; figure 2*a*).

Functional analysis can be considered as the output of canonical signalling. Figure 2*b* shows a broad number of functional pathways statistically significantly affected in MSCs by the two test topographies and by dexamethasone treatment. However, analysis of up- or downregulations within the pathways shows that the topographies have some specificity of action, whereas dexamethasone non-specifically stimulates all the pathways. Of particular note is that the topographies produce a balance of up- and downregulations in connective tissue development and function, and predominantly upregulation in skeletal and muscular system development. However, dexamethasone treatment results in the upregulation of both functional pathways (figure 2*b*).

By 28 days, none of the pathways highlighted at 14 days were noted in MSCs cultured on 3% : 3000 and with dexamethasone, but pathways associated with ERK were still noted in the cells cultured on 40 : 400 although to a non-statistically significant level (figure 3*a*). Also at 28 days of culture, fewer functional pathways were highlighted. Again the topographies showed more selectivity of pathways affected in the MSCs than dexamethasone treatment. In particular, the 3% : 3000 was not influencing pathways as diverse as nervous system development, cardiovascular development and general organ development at this later time point (figure 3*b*).

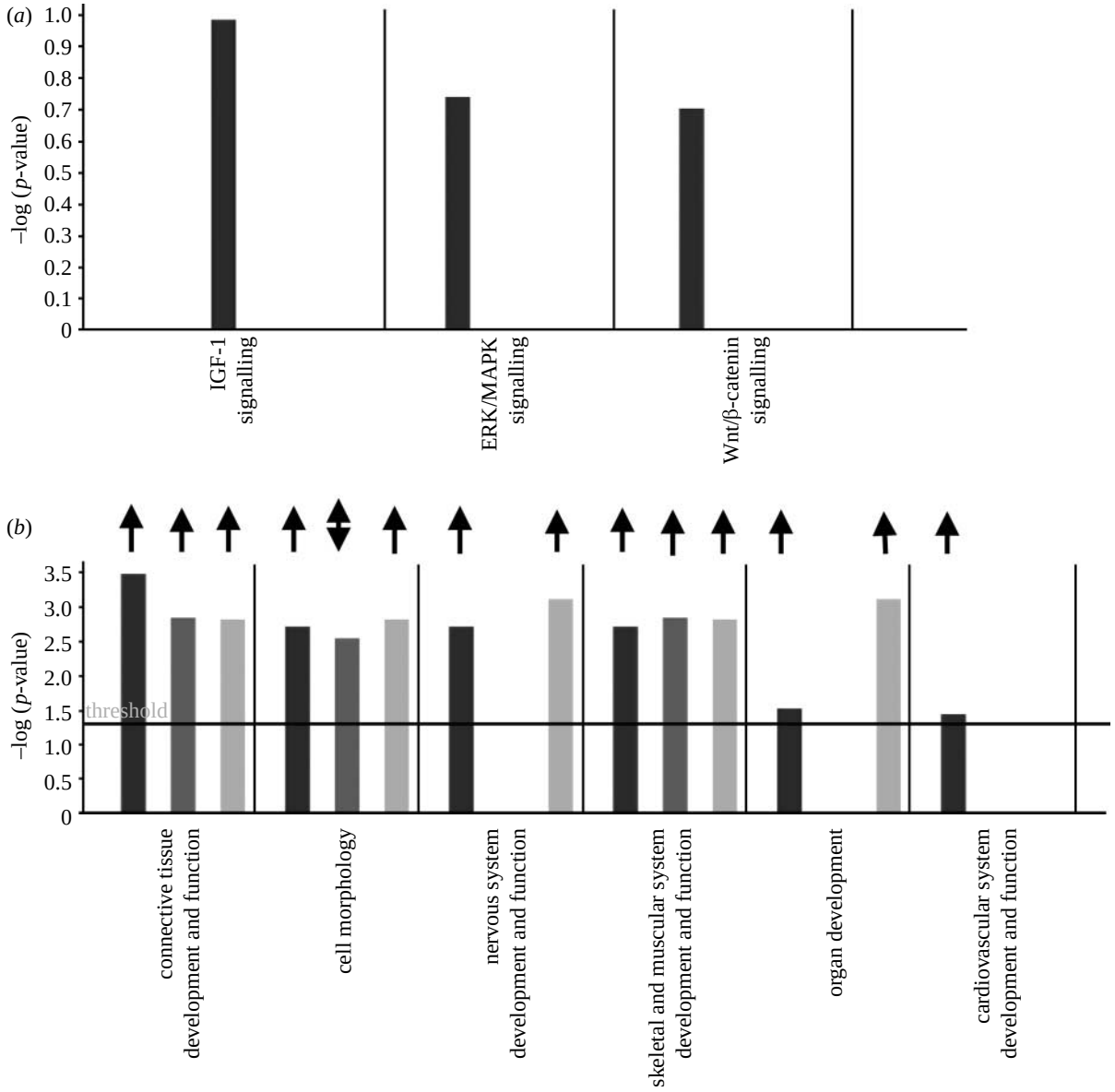

Figure 3. Ingenuity pathway analysis for MSCs cultured on the test topographies for 28 days. (*a*) Canonical pathway analysis for MSCs cultured on the 3% : 3000 and 40 : 400 test substrates compared with cells treated with dexamethasone. (*b*) Functional analysis showing a range of functional pathways active in cells in all growth conditions. Arrows indicate the trend of gene regulations within the pathway (up arrow, upregulations; double-headed arrow, balance of up- and downregulations; down arrow, downregulations). The threshold line shows the significance cut-off.

In an extension of the microarray analysis, 101 gene osteospecific arrays were used to compare mesenchymal stem cell differentiation for cells cultured on the test topographies and with dexamethasone (on planar material) with untreated cells cultured on planar control. The arrays demonstrated that cells cultured with dexamethasone displayed the highest levels of osteogenic upregulation (25 gene hits) followed by MSCs cultured on 3% : 3000 (15 gene hits) and 40 : 400 (11 gene hits). In contrast, the cells cultured on the planar control demonstrated only three gene hits. interestingly, genes upregulated in MSC on the test topographies included genes critical in osteoblast adhesion (intercellular adhesion molecule 1, ICAM1; integrin αM, ITGAM; integrin α1, ITGA1), collagenous matrix modelling and signalling (transforming growth factor receptor, TGFBR1; matrix metallopeptidase 8, MMP8; collagens, COL) and osteospecific matrix production and mineralization (BGLAP (or osteocalcin), alkaline phosphatase, ALPL; Diehn *et al.* 2003; table 1).

To test for endothelial characteristics, 101 gene endothelial-specific arrays were used. The arrays demonstrated that dexamethasone-treated cells produced only three hits, while untreated control cells produced seven hits. MSCs on 40 : 400 produced a result comparable to dexamethasone-treated cells with only two hits. The cells cultured on 3% : 3000 produced a result closer to that of control with five hits for genes, including TFPI2 (tissue factor pathway inhibitor 2), KIT, ALOX5 (arachidonate 5-lipoxygenase), IL6 (interleukin 6), ENPEP (glutamyl aminopeptidase), AZU1 (azurocidin) and RIPK1 (receptor (TNFRSF)-interacting serine-threonine kinase 1). All are implicated in the interaction of tissue and blood cells (table 2).

Table 1. Summary of osteospecific gene hits (number of positive hits for each test condition is shown), including a brief description of function derived from Stanford Source (Diehn *et al.* 2003).

osteoblast array gene hits for MSCs on test surfaces						
gene	full name	control	40 : 400	3% : 3000	DEX	function
TGFBR1	transforming growth factor beta receptor 1	2	3	3	3	cell signalling and differentiation
MMP8	matrix metalloprotease 8	1	3	3	3	matrix remodelling
ICAM1	intercellular adhesion molecule 1	0	3	3	3	cell–cell adhesion
BGLAP (osteocalcin)	bone Gla protein	0	3	2	3	bone-specific matrix protein
MGP	matrix Gla protein	0	0	1	2	associates with bone matrix
COL18A1	collagen 18	0	0	0	2	matrix protein
COL17A1	collagen 17	0	0	1	0	matrix protein
COL12A1	collagen 12	0	0	0	2	matrix protein
COL11A1	collagen 11	0	0	1	0	matrix protein
COL7A1	collagen 7	0	2	1	3	matrix protein
COL5A1	collagen 5	1	3	2	3	matrix protein
COL1A1	collagen 1	0	3	1	2	matrix protein
ALPL	alkaline phosphatase	0	3	0	3	phosphate homeostasis
AMBN	ameloblastin	0	0	0	1	enamel protein
ITGA1	integrin α1	0	3	3	3	cell–matrix adhesion
ITGA3	integrin α3	0	0	3	0	cell–matrix adhesion
ITGAM	integrin αM	0	0	0	1	cell–matrix adhesion
CSF2	colony-stimulating factor 2	0	1	0	3	cell differentiation
ALAP	type 1 tumour necrosis factor receptor-shedding aminopeptidase regulator	0	0	3	0	interacts with IL6
FGFR	fibroblast growth factor receptor	0	0	0	1	cell differentiation
CALCR	calcitonin receptor	0	0	0	1	G-protein signalling
EGFR	epidermal growth factor receptor	0	0	0	1	cell differentiation
BMP1	bone morphogenic protein 1	0	0	0	1	cell differentiation

4. DISCUSSION

It is clear that cells *in vivo* exist within a complex three-dimensional environment with nanotopography provided by surrounding matrix milieu, for example collagen banding (67 nm repeat pattern) and protein folding and microtopography as well as interactions with neighbouring cells and bone apatite (Gadegaard *et al.* 2003). Thus, it is of interest to try and harness such cues for *in vitro* tissue development and eventual use for the design of medical materials.

A key question in cell biology is that of tissue-specific cell differentiation and the mechanism controlling the process. The cells have the same genome and same transcription factor pool to drive gene regulation while cells in different parts of the body take on a vast array of different and distinct phenotypes (Getzenberg 1994). Thus, from the results, it is tempting to speculate that topography could be an important component in tissue-specific development through mechanotransductive pathways as will be discussed.

In recent years it has become self-evident that cells can use features such as filopodia (or microspikes), which have a tip diameter in the range of 50–100 nm, to gather and use spatial information. The cells can use filopodia to produce contact guidance with features as small as 10 nm high—around the size of a typical protein (Dalby *et al.* 2004*a–c*). In addition, it has also been observed that MSCs have an increased interaction with topography compared with differentiated cells like fibroblasts (Hart *et al.* 2007). This evidence that stem cells are exquisitely sensitive to their nanoenvironment adds further evidence that the topographical environment is important for tissue-specific differentiation.

In previous histochemical studies where osteocalcin and osteopontin were immunolocalized for using antibodies, it was observed that osteoprogenitor cells on the 40 : 400 surface produced nodules rich in osteocalcin, but with little osteopontin (Dalby *et al.* 2006*b*). However, osteoprogenitors cultured on the 3% : 3000 surface produced nodules rich in both osteocalcin and osteopontin (Dalby *et al.* 2006*a*). These results suggest that the 3% : 3000 surface is more osteoinductive than the 40 : 400 surface.

This current study has demonstrated that an in-depth pathway analysis reveals large differences between topographical and chemical (dexamethasone) stimulation. Dexamethasone treatment appears to be

Table 2. Summary of endothelial specific gene hits (number of positive hits for each test condition), including a brief description of function derived from Stanford Source (Diehn *et al.* 2003).

endothelial array gene hits for MSCs on test surfaces						
gene	full name	control	40 : 400	3% : 3000	DEX	function
TFPI2	tissue factor pathway inhibitor 2	3	3	3	3	plasmin-mediated matrix remodelling
KIT	KIT	3	0	2	0	transmembrane receptor for mast cell growth factor
ALOX5	arachidonate 5-lipoxygenase	1	0	2	0	synthesis of leukotrienes
IL6	interleukin 6	2	0	1	0	B-cell differentiation
ENPEP	glutamyl aminopeptidase	1	1	1	2	B-cell differentiation
AZU1	azurocidin 1	1	0	0	0	monocyte and fibroblast chemotactic glycoprotein
SELE	selectin E	0	0	0	1	mediates cell adhesion to the vasculature
RIPK1	receptor (TNFRSF)-interacting serine–threonine kinase 1	1	0	0	0	cell signalling

wide-ranging and unspecific in action with a broad number of canonical and functional pathways stimulated. The canonical pathways were stimulated only to small degrees with dexamethasone, but the broad changes in genomic regulations (mainly upregulations as shown by the dendrographs in figures S1 and S2, electronic supplementary material) did trigger a large number of functional pathways at both 14 and 28 days of culture.

The topographies, however, were more selective in the canonical pathways affected, but the targeted pathways tended to be significantly changed with both up- and downregulations implicated. The results indicate that actin cytoskeleton signalling and p38 MAPK signalling pathways are targeted by topographies at the micro- and nanolevels (i.e. both 40 : 400 and 3% : 3000). Integrin and ERK (MAPK) signalling pathways appear to be specifically targeted by the topography with only nanoscale dimensions (3% : 3000). That cells use filopodia, driven by actin and forming integrin-containing adhesions in response to nanotopography (Dalby *et al.* 2004*b*) tallies well with the specific activation of adhesion and cytoskeleton-related pathways (MAPKs are a signalling cascade influenced by the actin cytoskeleton; Burridge & Chrzanowska-Wodnicka 1996).

The guidance of filopodia by nanotopography and subsequent changes in cytoskeletal arrangements and signalling may alter mechanical forces within the cell. Such mechanisms have recently been described in fibroblasts cultured on topography whereby cytoskeletal rearrangements affect the interphase nucleus organization and genomic regulation (Dalby *et al.* 2007*a*,*b*). Such theories are developments of original work on mechanical force involvement in cell function. Examples include fibroblast traction being important in collagen morphogenesis and homeostasis (Harris *et al.* 1981; Brown *et al.* 1998; Eastwood *et al.* 1998) and involvement of compression in cartilage function (Guilak 1995).

It is further interesting that the topographies, through their selective influence of canonical signalling, affected the same functional pathways as dexametha-sone through its broad action. Again, however, the topographies lead to a balance of up- and downregulations in the functional pathways whereas dexamethasone treatment leads to a predominate, non-discriminate upregulation. A key goal in bone tissue engineering is to reduce soft-tissue formation and increase hard-tissue formation. At 14 days, the topographies produced a large number of downregulations in the connective tissue development pathways and predominantly upregulations in the skeletal system development pathways. Dexamethasone, however, produced only a non-specific upregulation.

By 28 days of culture, very few canonical pathways were being differentially regulated compared with planar control in the MSCs, with only a few non-statistically significant observations being made for the 40 : 400 material. Similarly, for the functional analysis at 28 days, while dexamethasone was still having a stimulatory effect and 40 : 400 was still influencing upregulations in some of the pathways, the 3% : 3000 material showed few changes compared with planar control.

These, and the previous histochemical results (Dalby *et al.* 2006*a*,*b*), fit in well with the original observations by Stein and Lian on the progression of osteogenic differentiation (Stein & Lian 1993). After initial adhesion and proliferation, pathways associated with cell differentiation and tissue formation are activated (around day 14 where we show most canonical and functional gene activity here). By day 21, osteocalcin- and osteonectin-rich nodules should be evident (as demonstrated on the test materials at 21 days of culture in Dalby *et al.* 2006*a*,*b*) and, by 28 days of culture, gene activity would be reduced as mineralization and matrix maintenance occur after the initial high levels of cellular activity.

While MSCs on both topographies appear to adhere approximately to this time course, it seems that the cells on the 3% : 3000 may have been encouraged to enter into osteogenic differentiation slightly faster than those on the 40 : 400 material and, once entering into the differentiation sequence, hold to the osteogenic time course. This is evidenced by an increased canonical

signalling at day 14 and a reduced signalling at day 28 in cell populations cultured on 3% : 3000 compared with those on 40 : 400. A second explanation may be that, due to the inherent plasticity of the stem cells, different proportions of the cells enter the osteoblastic lineage; hence, the high levels of functional output at day 14 on both test materials, yet the reduced osteospecific response when compared with dexamethasone treatment for cells on 40 : 400.

When considering the endothelial arrays, it is important to note that dexamethasone induced a paucity of gene hits, indicating that, while its action may be broad, endothelium is a phenotype suppressed by its other actions. The cells cultured on the nanotopographies did, however, show a degree of plasticity with a larger number of endothelial hits being observed, notably in cells cultured on the 3% : 3000 nanoislands. This variation in differentiation as a consequence of topography could have implications for tissue engineering, whereby replacement tissue could be cultured *in vitro* for transplantation *in vivo*. The ability to create surfaces that can deliver vascularized bone *in vitro* from autologous MSC would represent a significant advance.

In conclusion, it appears that the topographies produce a far more subtle and specific mode of action than dexamethasone, targeting a small number of canonical pathways (actin, integrin, p38 MAPK and ERK). Dexamethasone could, in fact, be considered a rather blunt tool in that it is efficient in stimulating stem cells, but does this by suppressing growth and switching many genes on non-specifically. The topographies, however, allow normal cell growth and proliferation, but promote osteogenic differentiation of the MSCs along the time-lines of classical differentiation studies. At the same time, they do not suppress endothelial differentiation.

There are other interesting material approaches as it has been shown that both material hardness and chemical/protein patterning can alter the differentiation of stem cells (Engler *et al.* 2004, 2006; McBeath *et al.* 2004). Topography, however, has the advantage as it is not easily removed like protein patterns and it does not affect material properties for the purpose as changing Young's modulus might. We also note that, when considering topography with serum-containing medium, questions of chemistry will also arise. It is our opinion that these topographies rather than changing interaction with serum proteins (to which the cells adhere) will simply change the presentation of the proteins to the cells.

It could thus be perceived that topography presents a preferable approach to stem cell modulation in bone tissue engineering than chemical or hormonal treatments. Understanding the mechanisms and controls therein is currently under investigation in our laboratories.

M.J.D. is a BBSRC David Phillips Fellow and this work was funded through this route. R.T. is supported by the BBSRC and R.O.C.O. is supported by BBSRC and EPSRC. We thank Prof. Adam Curtis, Prof. Chris Wilkinson and Dr Mathis Riehle for their useful discussions, Dr Nikolaj Gadegaard (Glasgow University) and Dr John Pedersen (SDC Dandisc A/S, Denmark) for the organizing and preparation of nickel shims and the Sir Henry Wellcome Functional Genomics Facility (IBLS, Glasgow University).

REFERENCES

Andersson, A.-S., Bäckhed, F., von Euler, A., Richter-Dahlfors, A., Sutherland, D. & Kasemo, B. 2003*a* Nanoscale features influence epithelial cell morphology and cytokine production. *Biomaterials* **24**, 3427–3436. (doi:10.1016/S0142-9612(03)00208-4)

Andersson, A.-S., Brink, J., Lidberg, U. & Sutherland, D. S. 2003*b* Influence of systematically varied nanoscale topography on the morphology of epithelial cells. *IEEE Trans. Nanobiosci.* **2**, 49–57. (doi:10.1109/TNB.2003.813934)

Andersson, A.-S., Olsson, P., Lidberg, U. & Sutherland, D. 2003*c* The effects of continuous and discontinuous groove edges on cell shape and alignment. *Exp. Cell Res.* **288**, 177–188. (doi:10.1016/S0014-4827(03)00159-9)

Bianco, P. & Robey, P. G. 2001 Stem cells in tissue engineering. *Nature* **414**, 118–121. (doi:10.1038/35102181)

Bianco, P., Riminucci, M., Gronthos, S. & Robey, P. G. 2001 Bone marrow stromal stem cells: nature, biology, and potential applications. *Stem Cells* **19**, 180–192. (doi:10.1634/stemcells.19-3-180)

Breitling, R., Armengaud, P., Amtmann, A. & Herzyk, P. 2004 Rank products: a simple, yet powerful, new method to detect differentially regulated genes in replicated microarray experiments. *FEBS Lett.* **573**, 83–92. (doi:10.1016/j.febslet.2004.07.055)

Brown, R. A., Prajapati, R., McGrouther, D. A., Yannas, I. V. & Eastwood, M. 1998 Tensional homeostasis in dermal fibroblasts: mechanical responses to mechanical loading in three-dimensional substrates. *J. Cell. Physiol.* **175**, 323–332. (doi:10.1002/(SICI)1097-4652(199806)175:3<323::AID-JCP10>3.0.CO;2-6)

Burridge, K. & Chrzanowska-Wodnicka, M. 1996 Focal adhesions, contractility, and signaling. *Annu. Rev. Cell Dev. Biol.* **12**, 463–518. (doi:10.1146/annurev.cellbio.12.1.463)

Clark, P., Connolly, P., Curtis, A. S., Dow, J. A. & Wilkinson, C. D. 1987 Topographical control of cell behaviour. I. Simple step cues. *Development* **99**, 439–448.

Clark, P., Connolly, P., Curtis, A. S., Dow, J. A. & Wilkinson, C. D. 1990 Topographical control of cell behaviour. II. Multiple grooved substrata. *Development* **108**, 635–644.

Clark, P., Connolly, P., Curtis, A. S., Dow, J. A. & Wilkinson, C. D. 1991 Cell guidance by ultrafine topography *in vitro*. *J. Cell Sci.* **99**(Pt 1), 73–77.

Cook, R., Wu, C. C., Kang, Y. J. & Han, J. 2007 The role of the p38 pathway in adaptive immunity. *Cell. Mol. Immunol.* **4**, 253–259.

Curtis, A. S. G. & Varde, M. 1964 Control of cell behaviour: topological factors. *J. Natl. Cancer Res. Inst.* **33**, 15–26.

Curtis, A. S. G. & Wilkinson, C. D. W. 2001 Nanotechniques and approaches in biotechnology. *Trends Biotechnol.* **19**, 97–101. (doi:10.1016/S0167-7799(00)01536-5)

Dai, Z., Li, Y., Quarles, L. D., Song, T., Pan, W., Zhou, H. & Xiao, Z. 2007 Resveratrol enhances proliferation and osteoblastic differentiation in human mesenchymal stem cells via ER-dependent ERK1/2 activation. *Phytomedicine* **14**, 806–814.

Dalby, M. J., Riehle, M. O., Johnstone, H., Affrossman, S. & Curtis, A. S. 2002*a* *In vitro* reaction of endothelial cells to polymer demixed nanotopography. *Biomaterials* **23**, 2945–2954. (doi:10.1016/S0142-9612(01)00424-0)

Dalby, M. J., Riehle, M. O., Johnstone, H. J., Affrossman, S. & Curtis, A. S. 2002*b* Polymer-demixed nanotopography: control of fibroblast spreading and proliferation. *Tissue Eng.* **8**, 1099–1108. (doi:10.1089/107632702320934191)

Dalby, M. J., Riehle, M. O., Yarwood, S. J., Wilkinson, C. D. & Curtis, A. S. 2003 Nucleus alignment and cell signaling in fibroblasts: response to a micro-grooved topography. *Exp. Cell. Res.* **284**, 274–282. (doi:10.1016/S0014-4827(02)00053-8)

Dalby, M. J., Gadegaard, N., Riehle, M. O., Wilkinson, C. D. & Curtis, A. S. 2004*a* Investigating filopodia sensing using arrays of defined nano-pits down to 35 nm diameter in size. *Int. J. Biochem. Cell Biol.* **36**, 2015–2025. (doi:10.1016/j.biocel.2004.03.001)

Dalby, M. J., Riehle, M. O., Johnstone, H., Affrossman, S. & Curtis, A. S. 2004*b* Investigating the limits of filopodial sensing: a brief report using SEM to image the interaction between 10 nm high nano-topography and fibroblast filopodia. *Cell Biol. Int.* **28**, 229–236. (doi:10.1016/j.cellbi.2003.12.004)

Dalby, M. J., Riehle, M. O., Sutherland, D. S., Agheli, H. & Curtis, A. S. 2004*c* Changes in fibroblast morphology in response to nano-columns produced by colloidal lithography. *Biomaterials* **25**, 5415–5422. (doi:10.1016/j.biomaterials.2003.12.049)

Dalby, M. J., Riehle, M. O., Sutherland, D. S., Agheli, H. & Curtis, A. S. 2004*d* Fibroblast response to a controlled nanoenvironment produced by colloidal lithography. *J. Biomed. Mater. Res. A* **69A**, 314–322. (doi:10.1002/jbm.a.20138)

Dalby, M. J., McCloy, D., Robertson, M., Agheli, H., Sutherland, D., Affrossman, S. & Oreffo, R. O. C. 2006*a* Osteoprogenitor response to semi-ordered and random nanotopographies. *Biomaterials* **27**, 2980–2987. (doi:10.1016/j.biomaterials.2006.01.010)

Dalby, M. J., McCloy, D., Robertson, M., Wilkinson, C. D. W. & Oreffo, R. O. C. 2006*b* Osteoprogenitor response to defined topographies with nanoscale depths. *Biomaterials* **27**, 1306–1315. (doi:10.1016/j.biomaterials.2005.08.028)

Dalby, M. J., Biggs, M. J. P., Gadegaard, N., Kalna, G., Wilkinson, C. D. W. & Curtis, A. S. G. 2007*a* Nanotopographical stimulation of mechanotransduction and changes in interphase centromere positioning. *J. Cell. Biochem.* **100**, 326–338. (doi:10.1002/jcb.21058)

Dalby, M. J., Gadegaard, N., Herzyk, P., Sutherland, D., Agheli, H., Wilkinson, C. D. W. & Curtis, A. S. G. 2007*b* Nanomechanotransduction and interphase nuclear organization influence on genomic control. *J. Cell. Biochem.* **102**, 1234–1244. (doi:10.1002/jcb.21354)

Diehn, M. *et al.* 2003 Source: a unified genomic resource of functional annotations, ontologies, and gene expression data. *Nucleic Acids Res.* **31**, 219–223. (doi:10.1093/nar/gkg014)

Eastwood, M., McGrouther, D. A. & Brown, R. A. 1998 Fibroblast responses to mechanical forces. *Proc. Inst. Mech. Eng.* **212**(Pt H), 85–92.

Eisen, M. B., Spellman, P. T., Brown, P. O. & Botstein, D. 1998 Cluster analysis and display of genome-wide expression patterns. *Proc. Natl Acad. Sci. USA* **95**, 14 863–14 868. (doi:10.1073/pnas.95.25.14863)

Engler, A. J., Griffin, M. A., Sen, S., Bonnemann, C. G., Sweeney, H. L. & Discher, D. E. 2004 Myotubes differentiate optimally on substrates with tissue-like stiffness: pathological implications for soft or stiff microenvironments. *J. Cell Biol.* **166**, 877–887. (doi:10.1083/jcb.200405004)

Engler, A. J., Sen, S., Sweeney, H. L. & Discher, D. E. 2006 Matrix elasticity directs stem cell lineage specification. *Cell* **126**, 677–689. (doi:10.1016/j.cell.2006.06.044)

Friedenstein, A. J. 1976 Precursor cells of mechanocytes. *Int. Rev. Cytol.* **47**, 327–359.

Gadegaard, N., Mosler, S. & Larsen, N. B. 2003 Biomimetic polymer nanostructures by injection moulding. *Macromol. Mater. Eng.* **288**, 76–83. (doi:10.1002/mame.200290037)

Getzenberg, R. H. 1994 Nuclear matrix and the regulation of gene expression: tissue specificity. *J. Cell. Biochem.* **55**, 22–31. (doi:10.1002/jcb.240550105)

Guilak, F. 1995 Compression-induced changes in the shape and volume of the chondrocyte nucleus. *J. Biomech.* **28**, 1529–1541. (doi:10.1016/0021-9290(95)00100-X)

Harris, A. K., Stopak, D. & Wild, P. 1981 Fibroblast traction as a mechanism for collagen morphogenesis. *Nature* **290**, 249–251. (doi:10.1038/290249a0)

Hart, A., Gadegaard, N., Wilkinson, C. D., Oreffo, R. O. C. & Dalby, M. J. 2007 Osteoprogenitor response to low-adhesion nanotopographies originally fabricated by electron beam lithography. *J. Mater. Sci. Mater. Med.* **18**, 1211–1218. (doi:10.1007/s10856-007-0157-7)

Howard, D., Partridge, K., Yang, X., Clarke, N. M. P., Okubo, Y., Bessho, K., Howdle, S. M., Shakesheff, K. M. & Oreffo, R. O. C. 2002 Immunoselection and adenoviral genetic modulation of human osteoprogenitors: *in vivo* bone formation on PLA scaffold. *Biochem. Biophys. Res. Commun.* **299**, 208–215. (doi:10.1016/S0006-291X(02)02561-5)

McBeath, R., Pirone, D. M., Nelson, C. M., Bhadriraju, K. & Chen, C. S. 2004 Cell shape, cytoskeletal tension, and RhoA regulate stem cell lineage commitment. *Dev. Cell* **6**, 483–495. (doi:10.1016/S1534-5807(04)00075-9)

Mirmalek-Sani, S. H., Tare, R. S., Morgan, S. M., Roach, H. I., Wilson, D. I., Hanley, N. A. & Oreffo, R. O. C. 2006 Characterization and multipotentiality of human fetal femur-derived cells—implications for skeletal tissue regeneration. *Stem Cells* **24**, 1042–1053. (doi:10.1634/stemcells.2005-0368)

Oreffo, R. O., Bord, S. & Triffitt, J. T. 1998 Skeletal progenitor cells and ageing human populations. *Clin. Sci. (Lond.)* **94**, 549–555.

Oreffo, R. O. C., Cooper, C., Mason, C. & Clements, M. 2005 Mesenchymal stem cells: lineage, plasticity and skeletal therapeutic potential. *Stem Cell Rev.* **1**, 169–178. (doi:10.1385/SCR:1:2:169)

Rajnicek, A. & McCaig, C. 1997 Guidance of CNS growth cones by substratum grooves and ridges: effects of inhibitors of the cytoskeleton, calcium channels and signal transduction pathways. *J. Cell Sci.* **110**(Pt 23), 2915–2924.

Rajnicek, A., Britland, S. & McCaig, C. 1997 Contact guidance of CNS neurites on grooved quartz: influence of groove dimensions, neuronal age and cell type. *J. Cell Sci.* **110**(Pt 23), 2905–2913.

Ruiz, C., Perez, E., Garcia-Martinez, O., Diaz-Rodriguez, L., Arroyo-Morales, M. & Reyes-Botella, C. 2007 Expression of cytokines IL-4, IL-12, IL-15, IL-18, and IFNgamma and modulation by different growth factors in cultured human osteoblast-like cells. *J. Bone Miner. Metab.* **25**, 286–292. (doi:10.1007/s00774-007-0767-7)

Stein, G. S. & Lian, J. B. 1993 Molecular mechanisms mediating proliferation/differentiation interrelationships during progressive development of the osteoblast phenotype. *Endocr. Rev.* **14**, 424–442. (doi:10.1210/er.14.4.424)

Triffitt, J. T. & Oreffo, R. O. C. 1998 Osteoblast lineage. In *Advances in organ biology: molecular and cellular biology of bone* (ed. M. Zaidi), pp. 475–498. Greenwich, CT: JAI Press, Inc.

Weiss, P. & Garber, B. 1952 Shape and movement of mesenchyme cells as functions of the physical structure of the medium. *Proc. Natl Acad. Sci. USA* **38**, 264–280. (doi:10.1073/pnas.38.3.264)

Wilkie, A. O. 2005 Bad bones, absent smell, selfish testes: the pleiotropic consequences of human FGF receptor mutations. *Cytokine Growth Factor Rev.* **16**, 187–203. (doi:10.1016/j.cytogfr.2005.03.001)

Wójciak-Stothard, B., Madeja, Z., Korohoda, W., Curtis, A. & Wilkinson, C. 1995 Activation of macrophage-like cells by multiple grooved substrata. Topographical control of cell behavior. *Cell Biol. Int.* **19**, 485–490. (doi:10.1006/cbir.1995.1092)

Wójciak-Stothard, B., Curtis, A., Monaghan, W., MacDonald, K. & Wilkinson, C. 1996 Guidance and activation of murine macrophages by nanometric scale topography. *Exp. Cell Res.* **223**, 426–435. (doi:10.1006/excr.1996.0098)

Yang, X., Tare, R. S., Partridge, K. A., Roach, H. I., Clarke, N. M. P., Howdle, S. M., Shakesheff, K. M. & Oreffo, R. O. C. 2003 Induction of human osteoprogenitor chemotaxis, proliferation, differentiation, and bone formation by osteoblast stimulating factor-1/pleiotrophin: osteoconductive biomimetic scaffolds for tissue engineering. *J. Bone Miner. Res.* **18**, 47–57. (doi:10.1359/jbmr.2003.18.1.47)